Journal of Neurology
https://doi.org/10.1007/s00415-024-12545-4

ORIGINAL COMMUNICATION

Hippocampal hub failure is linked to long-term memory impairment in anti-NMDA-receptor encephalitis: insights from structural connectome graph theoretical network analysis

André Hechler[1,2] · Joseph Kuchling[3,4] · Leonie Müller-Jensen[3] · Johanna Klag[3] · Friedemann Paul[3,4,5] · Harald Prüss[3,6] · Carsten Finke[1,3]

Received: 12 March 2024 / Revised: 22 June 2024 / Accepted: 26 June 2024

Abstract

Background Anti-*N*-methyl-D-aspartate receptor (NMDAR) encephalitis is characterized by distinct structural and functional brain alterations, predominantly affecting the medial temporal lobes and the hippocampus. Structural connectome analysis with graph-based investigations of network properties allows for an in-depth characterization of global and local network changes and their relationship with clinical deficits in NMDAR encephalitis.

Methods Structural networks from 61 NMDAR encephalitis patients in the post-acute stage (median time from acute hospital discharge: 18 months) and 61 age- and sex-matched healthy controls (HC) were analyzed using diffusion-weighted imaging (DWI)-based probabilistic anatomically constrained tractography and volumetry of a selection of subcortical and white matter brain volumes was performed. We calculated global, modular, and nodal graph measures with special focus on default-mode network, medial temporal lobe, and hippocampus. Pathologically altered metrics were investigated regarding their potential association with clinical course, disease severity, and cognitive outcome.

Results Patients with NMDAR encephalitis showed regular global graph metrics, but bilateral reductions of hippocampal node strength (left: $p=0.049$; right: $p=0.013$) and increased node strength of right precuneus ($p=0.013$) compared to HC. Betweenness centrality was decreased for left-sided entorhinal cortex ($p=0.042$) and left caudal middle frontal gyrus ($p=0.037$). Correlation analyses showed a significant association between reduced left hippocampal node strength and verbal long-term memory impairment ($p=0.021$). We found decreased left ($p=0.013$) and right ($p=0.001$) hippocampal volumes that were associated with hippocampal node strength (left $p=0.009$; right $p<0.001$).

Conclusions Focal network property changes of the medial temporal lobes indicate hippocampal hub failure that is associated with memory impairment in NMDAR encephalitis at the post-acute stage, while global structural network properties remain unaltered. Graph theory analysis provides new pathophysiological insight into structural network changes and their association with persistent cognitive deficits in NMDAR encephalitis.

Keywords Anti-*N*-Methyl-D-Aspartate receptor encephalitis · Diffusion-weighted MRI · Graph analysis · Human connectome

Abbreviations

ACT	Anatomically constrained tractography
ALFF	Amplitude of low-frequency fluctuation
APL	Average shortest path length
BC	Betweenness centrality
CC	Clustering coefficient
CMFG	Caudal middle frontal gyrus
CNS	Central nervous system
CSD	Constrained spherical deconvolution
DMN	Default mode network
DTI	Diffusion tensor imaging
DWI	Diffusion-weighted imaging
EC	Entorhinal cortex
FA	Fractional anisotropy
FLIRT	FMRIB's Linear Image Registration Tool

André Hechler, Joseph Kuchling are equally contributing first authors.

Extended author information available on the last page of the article

Published online: 08 July 2024

FOV	Field of view
HC	Healthy controls
HI	Hippocampus;
MD	Mean diffusivity
MS	Multiple sclerosis
MTL	Medial temporal lobe
NMDAR encephalitis	Anti-*N*-methyl-D-aspartate receptor encephalitis
PC	Participation coefficient (PC)
PCU	Precuneus
ROI	Region-of-interest
rs-fMRI	Resting state functional MRI
TE	Echo time
TI	Inversion time
TR	Repetition time

Introduction

Anti-N-methyl-D-aspartate receptor (NMDAR) encephalitis is an autoimmune encephalitis with a characteristic neuropsychiatric syndrome that can include behavioral changes, movement disorders, hallucinations, seizures, and cognitive deficits [1, 2]. Despite the frequently severe clinical course [3], routine MRI often appears unremarkable in 50–77% of patients [4].

By contrast, functional MRI analyses showed impaired connectivity between the hippocampus and the default mode network (DMN) that correlated with memory impairment [5]. Investigations of brain-wide functional networks demonstrated both widespread changes in the fronto-medial and fronto-parietal connections and focal disruptions within the medial temporal lobe (MTL) network, with the latter being closely associated with disease severity and memory performance [6]. Moreover, diffusion tensor imaging (DTI) investigations revealed widespread fractional anisotropy (FA) and mean diffusivity (MD) alterations that correlated with disease severity, reflecting profound structural white matter damage in NMDAR encephalitis [5]. In addition, brain-wide alterations in superficial white matter diffusivity were observed that were associated with disease severity and with persistent deficits of working memory, verbal memory, visuospatial memory, and attention [7]. Interestingly, patient-derived NMDAR antibodies have recently been shown to alter NMDA receptor function in oligodendrocytes, suggesting a link between antibody-mediated dysfunction of NMDARs in oligodendrocytes and white matter alterations detected using MRI analyses [8]. However, despite these functional network changes and structural white matter alterations, detailed investigations of structural connectivity and network efficiency changes caused by NMDAR encephalitis and their potential association with clinical and cognitive deficits are still missing.

Diffusion-weighted imaging (DWI)-based probabilistic tractography allows for a high-resolution reconstruction of white matter tracts within the whole brain [9]. These analyses have consistently identified central brain regions ("hubs") that are critically important for efficient brain communication given their role for the integration of distributed neural activity [10]. However, their high level of centrality also renders hubs particularly susceptible to disconnection and dysfunction. Indeed, graph theoretical analyses have identified dysfunction of a set of network parameters to be closely related to clinical and cognitive symptoms in multiple sclerosis (MS) [11, 12], neuromyelitis optica spectrum disorders [13], schizophrenia [14], and Alzheimer's disease [15, 16].

Here, we aimed to generate structural networks using an analysis pipeline of constrained spherical deconvolution (CSD)-based probabilistic tractography within the anatomically constrained tractography (ACT) framework [17–19] to evaluate global, modular, and nodal characteristics of structural networks from NMDAR encephalitis patients. We then correlated pathologically altered network metrics with clinical and cognitive measures to elucidate potential associations between structural network changes and clinical disability.

Methods

Participants

Sixty-one patients with NMDAR encephalitis in the post-acute stage (52 [86.9%] female patients; median age = 25 years [range 15–49 years]; median time from acute hospital discharge: 18 months; for further data see Table 1) were recruited from the Department of Neurology at Charité–Universitätsmedizin Berlin. Investigations comprised clinical evaluation, comprehensive neuropsychological assessment, and magnetic resonance imaging (MRI) data acquisition. Characteristic clinical presentation and detection of IgG NMDA receptor antibodies in the cerebrospinal fluid served as the basis for diagnosis according to current guidelines [2]. We enrolled 61 age- and sex-matched healthy participants without neurological or psychiatric diseases from our ongoing imaging database (EA4/011/19 and EA 1/163/12) to serve as healthy controls (HC). All participants gave written informed consent for all investigations and scientific publication of data prior to their inclusion in the study. The study was approved by the Charité ethics committee (EA4/011/19) and was performed in accordance with The Code of Ethics of the World Medical Association (1964 Declaration of Helsinki) in its currently applicable version.

Table 1 Clinical cohort description

	NMDAR encephalitis	Healthy controls
Sex, n (% female)	53 female/8 male [86.9%]	52 female/9 male [85.2%]
Age, yr, median ± SD (range)	25.5 ± 8.9 (15–49)	26.5 ± 8.7 (16–51)
Onset–treatment interval [d; median (IQR)]	19 (100)	–
Time since discharge from hospital [m; median (IQR)]	18.0 (24.0)	–
Acute-stage mRS [median (range)]	4 (2–5)	–
mRS at MRI [median (range)]	1 (0–3)	–
Tumor [n (%)]	12 (19.7%)	–

IQR interquartile range, *SD* standard deviation, *m* months, *yr* years, *d* days, *mRS* = modified Rankin scale

Neuropsychological assessment

All NMDAR encephalitis patients underwent comprehensive neuropsychological assessment as described in detail previously [20] using the following tests: the Test of Attentional Performance (TAP Version 2.3.1) [21] was used to assess selective, divided, and sustained attention. The German version of the Rey Auditory Verbal Learning Test (RAVLT)) [22, 23] was administered to measure verbal learning, immediate memory, recognition memory, and delayed recall. The Rey–Osterrieth Complex Figure Test (ROCF) [24, 25] was used to assess immediate and delayed recall visuospatial memory. A Go/No-Go paradigm and the Stroop Color and Word Test (SCWT) [26] were used to measure executive function, cognitive flexibility, and inhibitory control. The Stroop task, by origin and definition, primarily investigates inhibitory control and cognitive flexibility, i.e., executive functions [26]. Of note, activity in attention areas is observed during the performance of the Stroop [27], and previous studies suggested the application of the Stroop Task to other cognitive domains such as attention or working memory [28]. However, we used Stroop test to assess deficits in executive functioning, since these are among the core cognitive deficits in NMDARE [20, 29].

MRI acquisition

All MRI data were acquired on the same 3T scanner (Tim Trio Siemens, Erlangen, Germany) using a single-shot echo planar imaging sequence for diffusion MRI acquisition (repetition time [TR] = 7500 ms, echo time [TE] = 86 ms; field of view [FOV] = 240 × 240 mm; voxel size = 2.5 × 2.5 × 2.3 mm^3, 61 slices, 64 non-colinear directions, b-value = 1000 s/mm) and a volumetric high-resolution T1-weighted magnetization prepared rapid acquisition gradient echo (MPRAGE) sequence (TR/TE/inversion time [TI] = 1900/2.55/900 ms, FOV = 240 × 240 mm^2, matrix size = 240 × 240, 176 slices, slice thickness = 1 mm).

DWI preprocessing and anatomically constrained probabilistic tractography

DWI preprocessing and probabilistic tractography were performed using MRtrix3 [30], FMRIB Software Library's (FSL) [31], and Advanced Normalization Tools (ANTs) [32], according to a previously described protocol [17, 33] (Fig. 1). The preprocessing included denoising, eddy current correction, motion correction (using FSL topup), and bias-field correction (using ANTs). Structural T1 scans were parcellated into a total of 84 cortical and subcortical areas using the standard Freesurfer pipeline [34]. Tissue segmentation was performed using FSL FAST [35] as implemented in MRtrix3. Local fODF were obtained with probabilistic tractography using single-tissue CSD [18]. For improved streamline trajectories and rejection, we used ACT and limited seeding and termination to the interface of white matter and cortical or subcortical gray matter based on the segmented anatomical image [17].

Volumetric analysis

Analysis of a selection of regional subcortical and white matter brain volumes focusing on the volumes of the left and right hippocampus, the posterior cingulate cortex as a representative of the default mode network (DMN, using the usual seed region), and cerebral white matter as a global parameter was performed using volumetric segmentation with Freesurfer version 6.0 including the removal of non-brain tissue with a hybrid watershed/surface demarcation procedure and automated Talairach transformation, followed by segmentation of the cortical and subcortical volumetric structures [36].

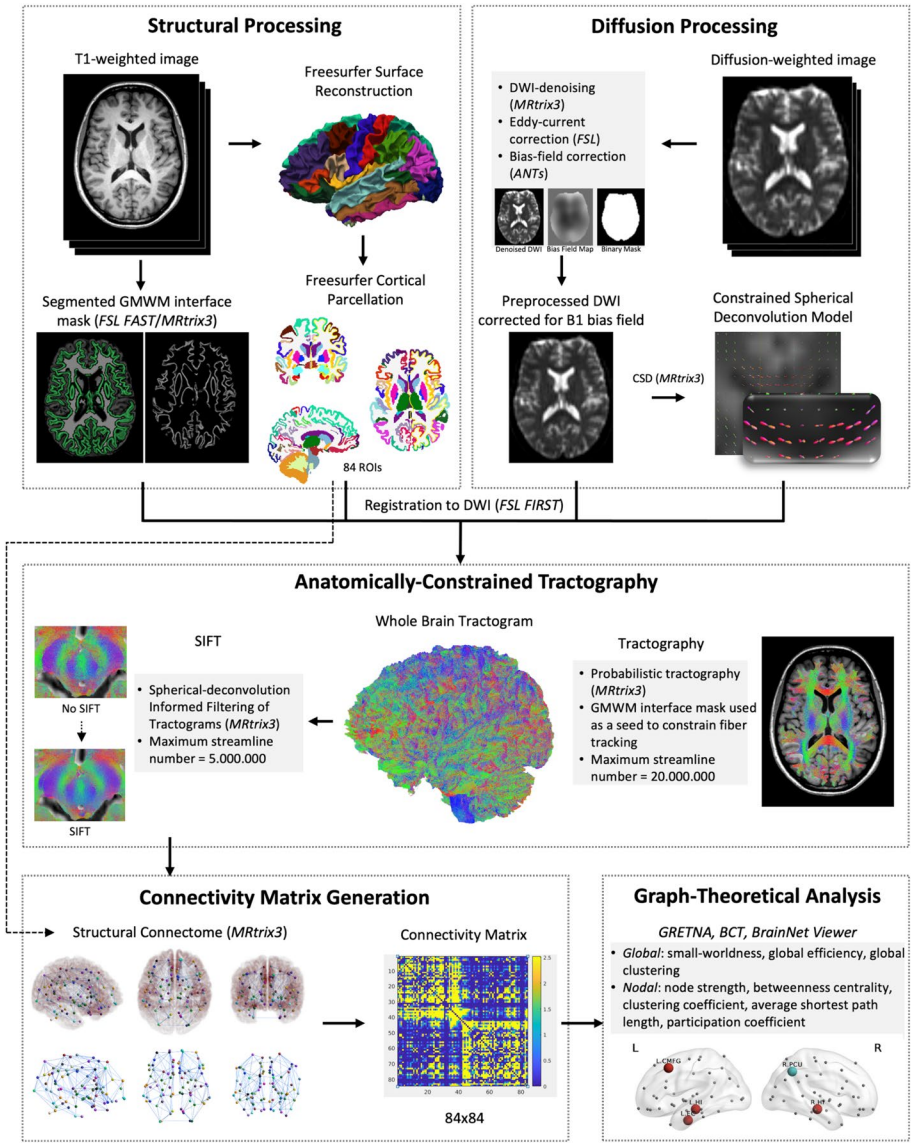

Fig. 1 Structural T1 scans were parcellated into a total of 84 cortical and subcortical areas. Tissue segmentation was performed using FSL FAST [35] to generate a gray matter–white matter (GMWM) interface mask as implemented in MRtrix3. Diffusion-weighted images (DWI) preprocessing included denoising, eddy current correction, motion correction and bias-field correction. Local fiber orientation density functions (fODF) were obtained using single-tissue CSD [18]. For improved streamline trajectories and rejection, we used anatomically-constrained tractography (ACT) [17]. We then filtered the tractogram using spherical deconvolution-based filtering of tractograms (SIFT) [37]. Structural connectivity matrices were created based on the results of ACT and SIFT with columns and rows corresponding to the 84 anatomical regions (nodes) and cells corresponding to the number of streamlines (edges) between pairs of nodes. We used the Graph Theoretical Network Analysis Toolbox (GRETNA) [38] and the Brain Connectivity Toolbox (BCT) [39] to carry out graph analyses. Graphs were visualized using BrainNet Viewer [40]. Small-worldness, global efficiency and global clustering coefficient were calculated for whole networks and node strength, betweenness centrality (BC), clustering coefficient (CC), average shortest path length (APL) and participation coefficient (PC) for all nodes

Volumes of all structures were adjusted for intracranial volume (ICV) using the following formula:

$$\text{Volume}_{\text{adjusted}} = \text{Volume}_{\text{observed}} - \beta\left[\text{slope from ICV vs regional volume regression}\right] \times \left(\text{ICV}_{\text{observed}} - \text{ICV}_{\text{sample mean}}\right)$$

We then filtered the tractogram using SIFT [37], which has been shown to improve the biological plausibility of

the reconstructed tracts by discarding streamlines that do not correspond well to the underlying diffusion signal [41]. To balance the risk of an overabundance of false positive fibers (weak filtering) against the risk of artificially sparse tractograms (strong filtering) and to address limitations of computational demand (large amounts of streamline creation or strong filtering), an overall 20 million streamlines were created and subsequently filtered down to 5 million streamlines, gaining connectome accuracy comparable to previously published literature [17, 37, 41].

Graph theory-based network analysis

Structural connectivity matrices were created based on the results of ACT and SIFT with columns and rows corresponding to the 84 anatomical regions (nodes) and cells corresponding to the number of streamlines (edges) between pairs of nodes. We used the Graph Theoretical Network Analysis Toolbox (GRETNA) [38] and the Brain Connectivity Toolbox (BCT) [39] to carry out graph analyses (see Fig. 1). Graphs were visualized using BrainNet Viewer [40]. Raw connectivity matrices contained a high number of edges with low probability, resulting in very dense networks that can distort classical graph measures [42]. Therefore, we integrated graph measures over a range of cutoffs (1% and 10% wiring cost in steps of 1% and thresholds between 10 and 90% in steps of 5%) as suggested previously [43]. A range of ten thresholds in steps of 5% connection density was chosen, with the upper bound defined as the most liberal threshold resulting in consistent small-worldness and the lower bound defined as the most conservative threshold that did not result in complete fragmentation of nodes. In our data, small-worldness (indicated by Sigma) showed marked variation over the complete range of thresholds (1–90% connection density), but low between-subject variability on individual levels. As networks lost consistent small-worldness upward of 55%, this was defined as the upper bound of the threshold range. For networks below 10% connection density, fragmented nodes (node strength of 0) occurred with increasing probability. Consequently, we chose 10% as the lower bound. All tests on graph metrics were carried out using the area under the curve (AuC) over the described threshold range.

We subsequently tested differences in nodal graph metrics on Freesurfer-based parcellation areas pertaining to the MTL (hippocampus, parahippocampal gyrus and entorhinal cortex) [44] and DMN (bilateral medial orbitofrontal gyrus, caudal medial frontal gyrus, caudal and rostral anterior cingulate, posterior cingulate, precuneus and inferior parietal gyrus) [45] since we expected marked network changes most likely to occur in these regions based on MR alterations observed in previous studies [5, 6, 46]. Small-worldness, global efficiency, and global clustering coefficient were calculated for whole networks and node strength, betweenness centrality (BC), clustering coefficient (CC), average shortest path length (APL), and participation coefficient (PC) for all nodes. Small-worldness was derived from the sigma coefficient with values above 1 indicating small-world properties. Nodes belonging to the MTL and DMN were tested for differences in node strength, BC, and CC. We additionally tested the connectivity within MTL and DMN by total node strength and mean APL.

Statistical analysis

Subsequent statistical analyses were performed using R Studio (RStudio Team, 2015). Group differences in nodal and modular parameters between patients and HC were tested with non-parametric resampling (10,000 iterations) using the resample package [47]. Graph parameters showing significant differences were included in linear mixed-effects model analyses with age and years of education as covariates to investigate potential correlations with clinical (acute-stage mRS [48], onset–treatment interval) and neuropsychological (RAVLT delayed recall, ROCF delayed recall, TAP go/no-go test) parameters. Brain volume comparison was conducted by use of unpaired t tests and subsequent exploratory correlation analyses between hippocampal volumes and graph metrics using Pearson correlations. For all statistical analyses, a p value of < 0.05 was regarded as significant. Due to the exploratory nature of group comparisons and correlation analyses, we refrained from correction for multiple testing [49].

Results

Nodal graph metrics: MTL and DMN

Node strength in patients was significantly reduced in both left ($p = 0.049$) and right ($p = 0.013$) hippocampus relative to controls (Fig. 2). A significant node strength increase was found within the right precuneus ($p = 0.013$). Differences in BC were found for the left caudal middle frontal gyrus ($p = 0.037$) and the left entorhinal cortex ($p = 0.042$), with lower values in NMDAR encephalitis patients (Fig. 2). In addition, NMDAR encephalitis patients showed increased average path for the left hippocampus ($p = 0.017$) and the right parahippocampal gyrus ($p = 0.026$), while no differences were found with respect to the nodal CC. For a comprehensive overview of nodal graph metrics in the DMN and MTL anatomical regions, see Supplementary Tables S 1–4.

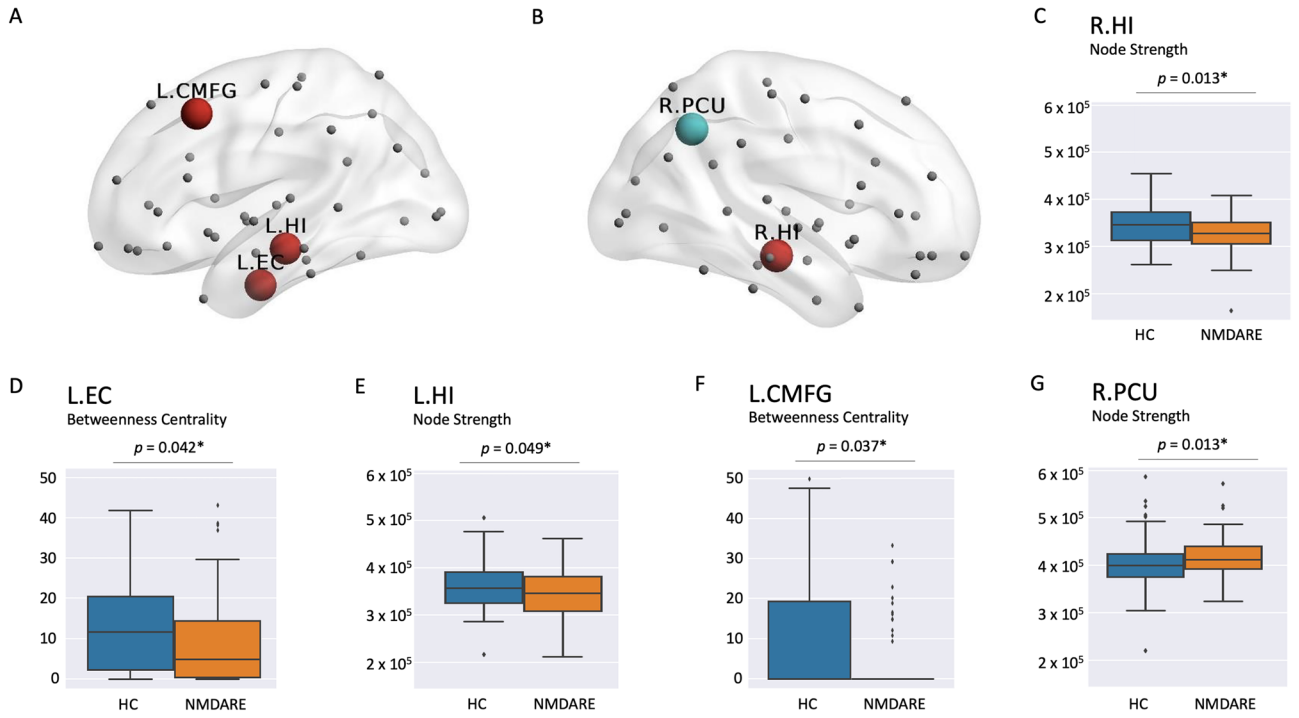

Fig. 2 **A**, **B** Lateral sagittal view with nodes exhibiting decreased (red) or increased (light blue) graph metrics in patients compared to HC. Red circles denote both decreases in node strength (L.HI, R.HI) or decreases in betweenness centrality (L.EC, L.CMFG). Light blue circles denote increases in node strength (R.PCU). **C–G** Illustration of comparative distribution of individual nodal graph metric values between HC (blue) and NMDAR encephalitis (orange) corresponding to the nodes highlighted in **A** and **B** is displayed in the boxplots below for each region of interest. For visualization purposes, extreme outliers are not shown but have been included in all analyses. *L.EC* left entorhinal cortex, *L.HI* left hippocampus, *L.CMFG* left caudal middle frontal gyrus, *R.HI* right hippocampus, *R.PCU* right precuneus

Modular graph metrics: MTL and DMN

The MTL showed a non-significant trend toward lower values for patients in total node strength on the left ($p = 0.09$) and right ($p = 0.08$) side and increased mean APL on the left side ($p = 0.05$; Table 2). No marked differences were found for any graph metric in the DMN (see Supplementary Table S5).

Global graph metrics

No significant differences in global efficiency and global clustering coefficient calculation were found between NMDAR encephalitis patients and HC (see Supplementary Table S6).

Correlation of graph metrics with clinical data

The following predictors were tested based on significant group differences: node strength of the left and right hippocampus and the right precuneus as well as BC of the left

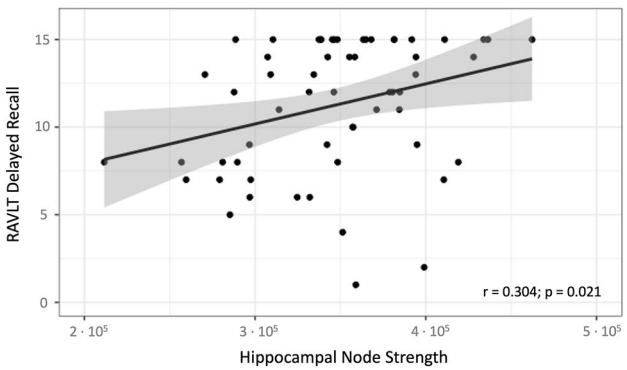

Fig. 3 Scatter plot of multiple linear regression analysis with individual values of left hippocampal node strength and RAVLT delayed recall values that showed a strong positive correlation (regression line; $r = 0.304$ [Pearson correlation coefficient]; p-value $= 0.021$ [corrected for age and years of education]). *RAVLT* Rey Auditory Verbal Learning Test

entorhinal cortex and the left caudal medial frontal cortex. Regarding clinical parameters, we found a significant

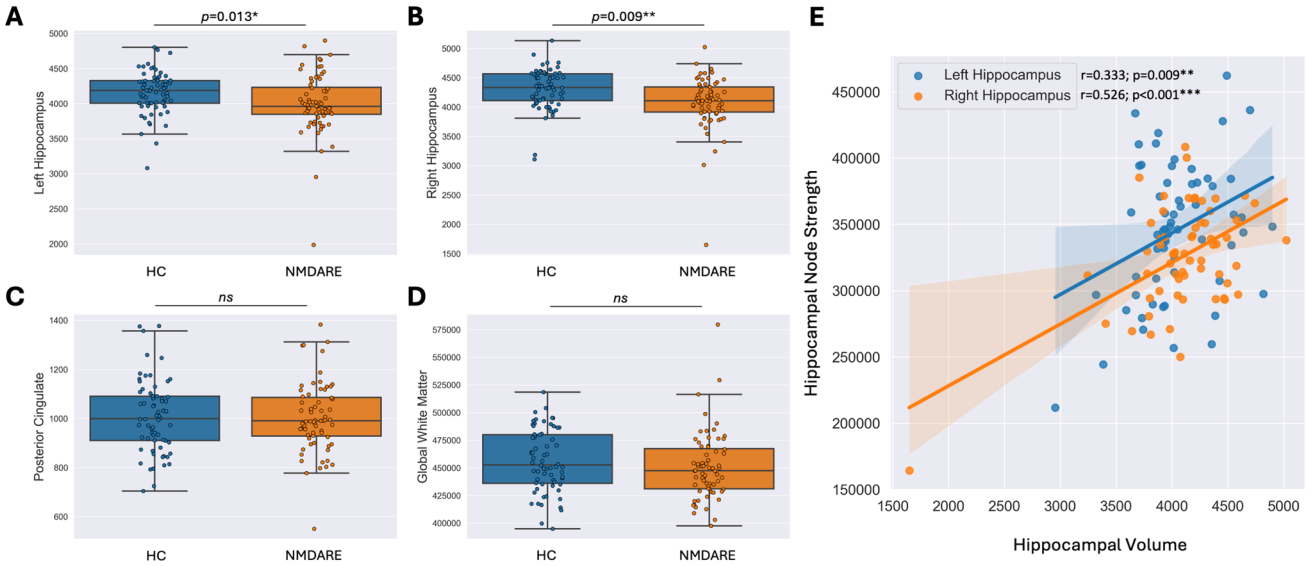

Fig. 4 Volumetric analysis and correlations between hippocampal volumes and node strength. Group differences in regional volume between NMDARE and HC were found in the **A** left hippocampus ($p=0.013$) and the **B** right hippocampus ($p=0.001$), while no significant group differences were observed in other brain regions, i.e. **C** posterior cingulate cortex and **D** global white matter volume. **E** An exploratory correlation analysis revealed strong correlations between left-sided hippocampal volume ($r=0.333$, $p=0.009$; orange) and right hippocampal volume ($r=0.526$, $p<0.001$; blue) and their respective node strengths.

association between the left hippocampal node strength and verbal long-term memory (RAVLT delayed recall test; $p=0.021$; Fig. 3). No other associations or significant correlations were observed.

Volumetric analysis

Volumetric analysis was conducted by assessing an a priori defined selection of regional volumes (Fig. 4). We found the left ($p=0.013$) and right hippocampus ($p=0.001$) to exhibit decreased gray matter volume in NMDARE patients compared to healthy controls. Hippocampal volumes were highly associated with hippocampal node strength (left hippocampus: $r=0.333$, $p=0.009$; right hippocampus: $r=0.526$, $p<0.001$). No further group differences or correlations were found.

Discussion

In this study, we investigated structural connectivity changes and multi-level network topology alterations in NMDAR encephalitis. To this end, we used an analysis framework with DWI-based probabilistic and anatomically constrained tractography and integration of graph metrics over multiple thresholds. We observed reduced node strength in both hippocampi, but increased node strength in the right precuneus in NMDAR encephalitis patients compared to healthy controls, indicating structural network reorganization following hippocampal hub failure. On a modular subnetwork level, we detected trends towards decreased node strength in the left and right MTL and increased path length for the left MTL in NMDAR encephalitis patients. Moreover, correlation analyses revealed an association between hippocampal node strength and verbal long-term memory in NMDAR encephalitis patients. By contrast, no significant differences in global network metrics were found between NMDAR encephalitis patients and HC. Overall, our study provides novel insights into structural connectivity disruptions at the modular and nodal levels and the impact of this network disintegration pattern on individual disease burden in NMDAR encephalitis.

The MTL is the key brain structure related to episodic memory, and damage to the MTL is associated with profound memory impairment [44, 50, 51]. Previous studies in NMDAR encephalitis patients reported on hippocampal atrophy and impaired microstructural integrity of the hippocampal formation that were correlated with memory deficits [5, 52]. Our structural network findings with bilateral reductions in hippocampal node strength, reduced BC in the left entorhinal cortex, and increased APL in the left hippocampus and right parahippocampal gyrus lend further support to the notion that hippocampal damage and associated structural network disruption play key roles in NMDAR encephalitis pathophysiology.

The connectivity architecture of the brain (the connectome) is characterized by a central core of highly

interconnected hub regions that are critical for efficient communication [53]. These network hubs are brain regions with high node strength (i.e., high number of connections [edges] with other nodes in the network) and betweenness centrality (i.e., high number of shortest paths in a network that pass through this node) [39]. However, given their crucial importance, hubs are strategic vulnerability points and damage to hubs leads to extensive network disruption and prominent clinical symptoms [53]. The hippocampus is one of the key hubs in the connectome given its high node strength and betweenness centrality. Here, we observed a bilateral reduction of hippocampal node strength in patients with NMDAR encephalitis. These results thus show that the disease targets a central network region of the brain, leading to disrupted hub function of the hippocampus and impaired connectivity of this densely connected brain structure [10]. Interestingly, this is in line with observations that other neurological disorders, including Alzheimer's disease, Parkinson's disease, and multiple sclerosis, are likewise associated with damage to highly connected hub nodes [16].

We found a strong association between hippocampal volumes and their respective node strengths. While the exact pathophysiological underpinnings of graph metric alterations, particularly node strength decrease, are still investigated and seem not to be specific to a particular type of pathophysiology, we propose two hypotheses. First, NMDAR antibodies lead to damage to hippocampal neurons, resulting in white matter tract degradation and reduction in fiber strength through Wallerian or trans-synaptic neurodegeneration [54]. This hypothesis could explain the correlation between hippocampal volume and node strength. Second, white matter damage may result from demyelination due to altered function of NMDARs in oligodendrocytes [8]. It is suggested that these altered NMDAR function might cause a decrease of expression of glucose transporter 1 (GLUT1) which metabolically supports axonal function, suggesting a link between antibody-mediated dysfunction of NMDARs in oligodendrocytes [8] and the reported widespread white matter alterations in NMDARE [5]. However, it remains unclear which mechanism is responsible for the correlation observed and to what extent the correlations can be seen as causative. Future longitudinal studies are therefore needed to explore potential causative relationships and mechanisms regarding hippocampal volumetric features and structural graph metrics. Of note, our findings demonstrate that hippocampal node strength correlates with regional hippocampal volume, and volumetric changes alone do not account for the full variance in structural changes. Node strengths of the left entorhinal cortex and left caudal middle frontal gyrus were altered without corresponding volumetric changes, indicating independent white matter damage, potentially caused by antibody-mediated dysfunction of oligodendrocyte NMDARs [8]. A recent study using diffusion-weighted imaging (DWI) in anti-leucine-rich, glioma-inactivated 1 encephalitis (LGI1-E) has shown both nodal and global structural changes, classifying LGI1-E as a network disease that impacts both limbic and extra-limbic systems [55]. These changes in LGI1-E substantially differ from the purely nodal network alterations that we report in NMDARE. Thus, network patterns derived from graph metrics offer additional informative value beyond morphometric data alone and may aid in the differential diagnosis and prognostic evaluation of autoimmune encephalitis in the future.

Our findings are in line with previous reports on bilateral atrophy of the input and output regions of the hippocampal circuit alongside microstructural damage in both hippocampi in NMDAR encephalitis [46]. Recent resting-state functional MRI investigations provided evidence on widespread functional connectivity impairment within distributed large-scale functional networks, including sensorimotor, frontoparietal, lateral–temporal, and visual networks [5, 6, 55, 56]. Here, we observed structural connectivity alterations affecting both hippocampi and areas outside MTL indicating that previously identified functional network changes might at least partially be based on these structural changes. These alterations are most likely caused by direct effects of anti-NMDAR antibodies on hippocampal neurons given their high density of NMDARs, eventually leading to substantial disruption of network topology with hippocampal hub failure [57].

Importantly, we observed a strong association between the left hippocampal node strength and verbal long-term memory. These findings are in line with previous functional MRI investigations that reported on impaired functional connectivity between the hippocampus and the default mode network (DMN) that correlated with verbal memory impairment in NMDAR encephalitis [5] and reports on close associations between focal disruptions within the MTL functional network and verbal memory scores in NMDAR encephalitis [6]. Hence, structural and functional connectome-based nodal hippocampal graph metrics might provide potential imaging markers of clinical relevance to assess cognitive status in NMDAR encephalitis in future studies. This is of particular importance, since cognitive deficits are the main contributor to long-term morbidity in NMDAR encephalitis and may either improve or persist over time in the individual patient depending on yet unknown recovery mechanisms [29]. While a decrease in hippocampal node strength was significantly associated with verbal memory impairment, we found that some patients achieved perfect scores on the RAVLT despite low hippocampal node strength. Thus, verbal memory impairment can only be partially explained by structural connectome damage. Other factors, such as hippocampal volume and compensatory mechanisms likely also influence cognitive performance, apart from pre-disease education level and age-related effects that were controlled for in our analyses.

In the MTL, we observed non-significant trends toward lower values in bilateral total node strength and an increased APL in the left MTL. The hippocampus serves as a critical hub within the MTL, and its structural connectivity with other regions, such as the entorhinal cortex and amygdala, forms a network crucial for integrating and processing information necessary for declarative memory and emotional regulation [58]. These trends support the view that white matter impairments have systemic, rather than regionally specific effects.

In addition, node strength of the right precuneus was significantly increased in NMDAR encephalitis patients. Previous anatomical and connectivity data suggest a central role for the precuneus in a wide range of higher-order cognitive functions and highly integrated tasks including reflective, self-related processing, emotion-related information processing, and episodic memory [59]. The precuneus is a core region of the DMN and is highly interconnected with the hippocampus [60, 61]. It shows reliable increases in activation during both rest and specific tasks and involvement in self-related mental representations during rest. Consequently, it has been proposed that the precuneus is involved in the network correlates of self-consciousness [62]. Hence, structural changes affecting the precuneus may contribute to episodic memory impairment and psychosocial symptoms including decreased judgment of the mental self [59]. However, future studies investigating potential associations between specific neuropsychiatric symptoms such as self-esteem and both functional and structural connectivity of the precuneus are highly warranted.

Our findings complement previous voxel-wise analyses of hippocampal connectivity in 43 NMDAR encephalitis patients that showed reduced functional connectivity between the hippocampus and precuneus [6]. Another resting-state fMRI study of 17 NMDAR encephalitis patients and 18 matched HC observed decreased amplitude of low-frequency fluctuation (ALFF) in patients in the left precuneus, indicating a decrease in spontaneous neural activity and precuneus functional impairment [63]. In addition, FDG-PET imaging revealed precuneus hypometabolism in six NMDAR encephalitis patients [64]. A recent study using [^{18}F]GE-179 PET identified a reduction in the density of open, active NMDARs in the anterior temporal lobes, superior parietal cortices and in the precuneus [65], lending further support to the notion of functional impairment of the precuneus in NMDAR encephalitis.

However, there is only limited data on structural connectivity of the precuneus. Our findings of increased precuneus node strength indicate a relative hyperconnectivity. Indeed, recently discussed mechanisms of compensatory remyelination after inflammatory brain damage might—at least partially—account for increased precuneus node strength in NMDAR encephalitis [66, 67]. Alternatively, precuneus node strength increase could be caused by plastic network reorganization given the nature of structural connectome properties and their potential response to acute disease damage. Structural reorganization mechanisms could feature local rerouting that can be thought of as a local outgrowth of new connections due to the diminished capacity of the affected hippocampal hubs, previously referred to as ‘hub failure’ [16].

Hub nodes in brain networks, such as the hippocampus, are highly connected areas that handle significant network traffic [10]. The "hub overload and failure" scenario [16] begins with one or more lesions, causing a redistribution of network traffic. In NMDARE, hippocampal dysfunction caused by NMDAR antibodies can lead to early hub overload and eventual failure. This results in reduced connectivity, atrophy, and disrupted cognitive function. We found bilateral hippocampal node strength decrease and atrophy as well as a trend for MTL network property change on a model level consistent with this “hub failure” hypothesis. In NMDARE, hippocampal damage would then lead to mid- to long-term redistribution of structural connectivity to other hubs. This redistribution is proportional to the connectivity of the affected nodes, with highly connected hubs like the precuneus and posterior cingulum taking on the largest share of the increased load. Of interest, we indeed observed increased precuneus node strength, indicating a network rerouting with increased load taken over by the precuneus, hence supporting the hub failure hypothesis [68] to occur in NMDARE. However, future longitudinal studies investigating network properties in the acute, post-acute, and long-term stages of the disease are necessary to characterize potential hub failure development in detail. Moreover, future translational MR studies in murine NMDAR antibody-associated disease models [69] may provide additional insights into potential histopathological correlates of these structural hyperconnectivities.

We observed a consistent trend toward lower node strengths in the left and right MTL and a trend for increased mean APL in the left MTL. By contrast, the DMN showed no changes in connectivity on the modular level. Our findings complement previous rs-fMRI analysis that did not detect functional connectivity changes within the DMN itself, but rather a decoupling between DMN and MTL [6]. Correspondence between modular network characteristics in structural and functional connectivity with positive correlations of edge weights between methods have been recently postulated and observed in healthy participants [70, 71]. In addition, rs-fMRI-based functional connectivity disruption might closely reflect similar structural connectivity degradation in the DMN [72], lending further support to consistent findings across imaging modalities.

As expected, we did not observe differences between NMDAR encephalitis and HC in global measures of network

topology. This is in line with findings in schizophrenia that similarly showed nodal and modular structural network changes, including longer node-specific path lengths of the bilateral frontal cortex and temporal pole regions, without significant alterations in global network properties [14]. Likewise, functional global network properties were shown to be unaltered in comatose patients when compared with healthy controls [73]. Interestingly, despite the lack of global network alterations in comatose patients, a further in-depth investigation revealed a marked reorganization on the nodal level with reduced hubness of occipital cortex nodes and abnormally increased hubness of nodes in the prefrontal and lateral parietal cortex [73]. Our findings, i.e., the absence of global network alterations in the context of specific alterations on the modular and nodal scale, are in agreement with these previous observations, indicating that modular and nodal changes predominate the structural connectome alterations in NMDAR encephalitis.

We report on the first use of DWI-based probabilistic tractography and subsequent whole brain connectome generation with graph theory analysis to assess the structural damage in NMDARE patients. DWI, combined with structural connectome and graph theory analysis, provides quantitative data that complement the qualitative assessments of routine MRI sequences. This allows for more precise and accurate measurements and both inter-individual and intra-individual comparisons over time. Hence, DWI might be particularly useful for monitoring disease progression and treatment response in individual patients as well as comparing data across different patient populations. Additionally, DWI facilitates tractography, i.e., the reconstruction of white matter fiber tracts, and subsequent analyses including whole brain tractography and structural connectome generation to assess complex white matter networks and their potential alterations due to specific disease pathology [74]. By contrast, the T1/T2 ratio is derived from routine T1- and T2-weighted clinical MRI sequences, and has shown high sensitivity in detecting microstructural changes correlating with cognitive performance in NMDAR encephalitis [75] without the necessity of further experimental sequences (such as DWI). The T1/T2 ratio could therefore be used for monitoring brain damage correlated with cognitive deficits in patients with NMDAR encephalitis without requiring additional scanning time. Future studies with cross-validation of different imaging methods are warranted to assess the capacity of T1/T2 ratio, but also DWI-based graph metrics to detect and monitor structural brain damage in NMDARE.

Limitations

Patients were studied during the post-acute stage rather than the acute stage of the disease. This time point enabled us to investigate the mid- to long-term processes that occur following acute NMDARE, specifically disease-mediated damage and compensatory connectivity reorganization. These processes are critical for understanding the persistent cognitive deficits often observed in NMDARE patients [29, 76]. Moreover, the deduction of potential compensatory mechanisms following the acute stage of NMDARE, which may lead to the structural connectome changes observed in our study, is limited by the cross-sectional design of our study. Thus, we cannot make inferences about the longitudinal course of structural connectivity features in NMDARE. Due to the investigations at the post-acute stage, our NMDARE patient cohort was characterized by relatively low mRS scores (median = 1; range 0–3) consistent with previous reports on post-acute stage NMDARE [29], while still exhibiting relevant cognitive deficits. In addition, we cannot exclude the presence of global network changes during the acute stages of NMDAR encephalitis. Due to time constraints inherent to clinical research, we used a limited set of neuropsychological tests to address the core cognitive deficits reported in NMDARE [20, 29]. DWI acquisition was limited to a b-value of 1000, exclusively allowing for single-tissue CSD model creation. While CSD-based probabilistic tractography still outperforms deterministic variants [77] at this level, a b-value of 3000 with subsequent multi-shell multi-tissue CSD has been suggested to further minimize the detrimental effects on tractogram construction [78].

Conclusion

We employed advanced tractography and graph theoretical methods to investigate the structural connectivity networks in NMDAR encephalitis. Our results reveal that medial temporal lobe structures, specifically the hippocampus, exhibit impaired connectivity, while higher-level network topology remains unaffected. Our study provides further evidence for the specific vulnerability of the hippocampus in NMDAR encephalitis, leading to a critical network hub failure. The correlation of hippocampal node strength with verbal memory performance suggests that structural hippocampal graph metrics may serve as potential MRI markers for assessing cognitive function in the post-acute stage of the disease. Future studies in larger NMDAR encephalitis populations at the acute and post-acute disease stage are warranted to evaluate the clinical utility of diffusion-weighted imaging-based structural connectivity and graph theoretical analysis for disease monitoring in individual patients.

Supplementary Information The online version contains supplementary material available at https://doi.org/10.1007/s00415-024-12545-4.

Acknowledgements We thank Susan Pikol and Cynthia Kraut for their excellent technical support. This work was supported by the German

Research Foundation (Clinical Research Unit KFO 5023 'BecauseY'/ Project number 504745852).

Author contributions Conceptualization: André Hechler, Joseph Kuchling, Carsten Finke. Methodology: André Hechler, Joseph Kuchling, Leonie Müller-Jensen. Formal analysis and investigation: André Hechler, Joseph Kuchling. Data curation: Leonie Müller-Jensen, Johanna Klag, André Hechler, Joseph Kuchling. Writing—original draft preparation: André Hechler, Joseph Kuchling. Writing—review and editing: Carsten Finke, Harald Prüss, Friedemann Paul, Leonie Müller-Jensen, Johanna Klag. Visualization: André Hechler, Joseph Kuchling. Funding acquisition: Carsten Finke, Harald Prüss. Resources: Carsten Finke, Harald Prüss, Friedemann Paul. Supervision: Carsten Finke.

Funding Open Access funding enabled and organized by Projekt DEAL. Funded by the Deutsche Forschungsgemeinschaft (DFG, German Research Foundation; Grant numbers FI 2309/1–1 and FI 2309/2–1 to C.F., FOR3004, PR 1274/2–1, PR 1274/3–1, and PR 1274/5–1 to H.P., by the Helmholtz Association (HIL-A03 to H.P.) and the German Ministry of Education and Research (BMBF; 01GM1908D to H.P.). JKu was participant in the BIH Charité (Junior) (Digital) Clinician Scientist Program funded by the Charité–Universitätsmedizin Berlin and the Berlin Institute of Health at Charité (BIH).

Data availability The data that support the findings of this study are available on request from the corresponding author. The data are not publicly available due to ethical restrictions.

Declarations

Conflicts of interest The authors declare that they have no conflict of interest.

Ethics approval The study was approved by the Charité ethics committee (EA4/011/19) and was performed in accordance with The Code of Ethics of the World Medical Association (1964 Declaration of Helsinki) in its currently applicable version.

Consent to participate All participants gave written informed consent for all investigations and scientific publication of data prior to their inclusion in the study.

References

1. Dalmau J, Tüzün E, Wu H et al (2008) Paraneoplastic anti–N-methyl-D-aspartate receptor encephalitis associated with ovarian teratoma. Ann Neurol 61:25–36
2. Graus F, Titulaer MJ, Balu R et al (2016) A clinical approach to diagnosis of autoimmune encephalitis. Lancet Neurol 15:391–404. https://doi.org/10.1016/S1474-4422(15)00401-9
3. Dalmau J, Lancaster E, Martinez-Hernandez E et al (2011) Clinical experience and laboratory investigations in patients with anti-NMDAR encephalitis. Lancet Neurol 10:63–74. https://doi.org/10.1016/S1474-4422(10)70253-2
4. Heine J, Prüss H, Bartsch T et al (2015) Imaging of autoimmune encephalitis–Relevance for clinical practice and hippocampal function. Neuroscience 309:68–83. https://doi.org/10.1016/j.neuroscience.2015.05.037
5. Finke C, Kopp UA, Scheel M et al (2013) Functional and structural brain changes in anti-N-methyl-D-aspartate receptor encephalitis. Ann Neurol 74:284–296. https://doi.org/10.1002/ana.23932
6. Peer M, Prüss H, Ben-Dayan I et al (2017) Functional connectivity of large-scale brain networks in patients with anti-NMDA receptor encephalitis: an observational study. Lancet Psychiatry 4:768–774. https://doi.org/10.1016/S2215-0366(17)30330-9
7. Phillips OR, Joshi SH, Narr KL et al (2018) Superficial white matter damage in anti-NMDA receptor encephalitis. J Neurol Neurosurg Psychiatry 89:518–525. https://doi.org/10.1136/jnnp-2017-316822
8. Matute C, Palma A, Serrano-Regal MP et al (2020) N-methyl-D-aspartate receptor antibodies in autoimmune encephalopathy alter oligodendrocyte function. Ann Neurol 87:670–676. https://doi.org/10.1002/ana.25699
9. Behrens TEJ, Woolrich MW, Jenkinson M et al (2003) Characterization and propagation of uncertainty in diffusion-weighted MR imaging. Magn Reson Med 50:1077–1088. https://doi.org/10.1002/mrm.10609
10. van den Heuvel MP, Sporns O (2013) Network hubs in the human brain. Trends Cogn Sci 17:683–696. https://doi.org/10.1016/j.tics.2013.09.012
11. He Y, Dagher A, Chen Z et al (2009) Impaired small-world efficiency in structural cortical networks in multiple sclerosis associated with white matter lesion load. Brain 132:3366–3379. https://doi.org/10.1093/brain/awp089
12. Stellmann J-P, Hodecker S, Cheng B et al (2017) Reduced rich-club connectivity is related to disability in primary progressive MS. Neurol Neuroimmunol Neuroinflammation 4:e375. https://doi.org/10.1212/NXI.0000000000000375
13. Chien C, Oertel FC, Siebert N et al (2019) Imaging markers of disability in aquaporin-4 immunoglobulin G seropositive neuromyelitis optica: a graph theory study. Brain Commun. https://doi.org/10.1093/braincomms/fcz026
14. van den Heuvel MP, Mandl RCW, Stam CJ et al (2010) aberrant frontal and temporal complex network structure in schizophrenia: a graph theoretical analysis. J Neurosci 30:15915–15926. https://doi.org/10.1523/JNEUROSCI.2874-10.2010
15. Lo C-Y, Wang P-N, Chou K-H et al (2010) Diffusion tensor tractography reveals abnormal topological organization in structural cortical networks in Alzheimer's disease. J Neurosci 30:16876–16885. https://doi.org/10.1523/JNEUROSCI.4136-10.2010
16. Stam CJ (2014) Modern network science of neurological disorders. Nat Rev Neurosci 15:683–695. https://doi.org/10.1038/nrn3801
17. Smith RE, Tournier J-D, Calamante F, Connelly A (2012) Anatomically-constrained tractography: Improved diffusion MRI streamlines tractography through effective use of anatomical information. Neuroimage 62:1924–1938. https://doi.org/10.1016/j.neuroimage.2012.06.005
18. Tournier J-D, Calamante F, Connelly A (2007) Robust determination of the fibre orientation distribution in diffusion MRI: Non-negativity constrained super-resolved spherical deconvolution. Neuroimage 35:1459–1472. https://doi.org/10.1016/j.neuroimage.2007.02.016

19. Tournier J-D, Calamante F, Gadian DG, Connelly A (2004) Direct estimation of the fiber orientation density function from diffusion-weighted MRI data using spherical deconvolution. Neuroimage 23:1176–1185. https://doi.org/10.1016/j.neuroimage.2004.07.037
20. Finke C, Kopp UA, Prüss H et al (2012) Cognitive deficits following anti-NMDA receptor encephalitis. J Neurol Neurosurg Psychiatry 83:195–198. https://doi.org/10.1136/jnnp-2011-300411
21. Zimmermann P, Fimm B (2017) Testbatterie zur Aufmerksamkeitsprüfung Version 2.3.1. Psychologische Testsysteme
22. Schmidt M (1996) Rey auditory verbal learning test: a handbook. Western Psychological Services, Los Angeles
23. Spreen O, Strauss E (1998) A compendium of neuropsychological tests: administration, norms, and commentary. Oxford University Press, New York
24. Osterrieth PA (1944) Le test de copie d'une figure complexe; contribution à l'étude de la perception et de la mémoire. [Test of copying a complex figure; contribution to the study of perception and memory]. Arch Psychol 30:206–356
25. Rey A (1941) L'examen psychologique dans les cas d'encéphalopathie traumatique. (Les problems.) [The psychological examination in cases of traumatic encepholopathy. Problems]. Arch Psychol 28:215–285
26. Stroop JR (1935) Studies of interference in serial verbal reactions. J Exp Psychol 18:643–662
27. Banich MT, Milham MP, Atchley R et al (2000) fMri studies of Stroop tasks reveal unique roles of anterior and posterior brain systems in attentional selection. J Cogn Neurosci 12:988–1000. https://doi.org/10.1162/08989290051137521
28. Scarpina F, Tagini S (2017) The stroop color and word test. Front Psychol. https://doi.org/10.3389/fpsyg.2017.00557
29. Heine J, Kopp UA, Klag J et al (2021) Long-term cognitive outcome in anti-NMDA receptor encephalitis. Ann Neurol. https://doi.org/10.1002/ana.26241
30. Tournier J-D, Smith R, Raffelt D et al (2019) MRtrix3: a fast, flexible and open software framework for medical image processing and visualisation. Neuroimage. https://doi.org/10.1016/j.neuroimage.2019.116137
31. Jenkinson M, Beckmann C, Behrens TEJ et al (2012) FSL NeuroImage 62:782–790
32. Avants BB, Tustison N, Song G (2011) Advanced Normalization Tools (ANTS). University of Pennsylvania, Penn Image Computing and Science Laboratory
33. Oldham S, ArnatkevičiūtėSmith ARE et al (2020) The efficacy of different preprocessing steps in reducing motion-related confounds in diffusion MRI connectomics. Neuroimage 222:117252. https://doi.org/10.1016/j.neuroimage.2020.117252
34. Fischl B (2004) Automatically parcellating the human cerebral cortex. Cereb Cortex 14:11–22. https://doi.org/10.1093/cercor/bhg087
35. Zhang Y, Brady M, Smith S (2001) Segmentation of brain MR images through a hidden Markov random field model and the expectation-maximization algorithm. IEEE Trans Med Imaging 20:45–57. https://doi.org/10.1109/42.906424
36. Fischl B, Salat DH, Busa E et al (2002) Whole brain segmentation: automated labeling of neuroanatomical structures in the human brain. Neuron 33:341–355. https://doi.org/10.1016/s0896-6273(02)00569-x
37. Smith RE, Tournier J-D, Calamante F, Connelly A (2013) SIFT: Spherical-deconvolution informed filtering of tractograms. Neuroimage 67:298–312. https://doi.org/10.1016/j.neuroimage.2012.11.049
38. Wang J, Wang X, Xia M et al (2015) GRETNA: a graph theoretical network analysis toolbox for imaging connectomics. Front Hum Neurosci 9:386. https://doi.org/10.3389/fnhum.2015.00386
39. Rubinov M, Sporns O (2010) Complex network measures of brain connectivity: Uses and interpretations. Neuroimage 52:1059–1069. https://doi.org/10.1016/j.neuroimage.2009.10.003
40. Xia M, Wang J, He Y (2013) BrainNet Viewer: a network visualization tool for human brain connectomics. PLoS ONE 8:e68910–e68910. https://doi.org/10.1371/journal.pone.0068910
41. Smith RE, Tournier J-D, Calamante F, Connelly A (2015) The effects of SIFT on the reproducibility and biological accuracy of the structural connectome. Neuroimage 104:253–265. https://doi.org/10.1016/j.neuroimage.2014.10.004
42. Yeh C-H, Smith RE, Liang X et al (2016) Correction for diffusion MRI fibre tracking biases: The consequences for structural connectomic metrics. Neuroimage 142:150–162. https://doi.org/10.1016/j.neuroimage.2016.05.047
43. Ginestet CE, Nichols TE, Bullmore ET, Simmons A (2011) Brain network analysis: separating cost from topology using cost-integration. PLoS ONE 6:e21570. https://doi.org/10.1371/journal.pone.0021570
44. Squire LR, Stark CEL, Clark RE (2004) THE medial temporal lobe. Annu Rev Neurosci 27:279–306. https://doi.org/10.1146/annurev.neuro.27.070203.144130
45. Raichle ME (2015) The brain's default mode network. Annu Rev Neurosci 38:433–447. https://doi.org/10.1146/annurev-neuro-071013-014030
46. Finke C, Kopp UA, Pajkert A et al (2016) Structural hippocampal damage following anti-N-methyl-D-aspartate receptor encephalitis. Biol Psychiatry 79:727–734. https://doi.org/10.1016/j.biopsych.2015.02.024
47. Hesterberg T (2015) resample: Resampling functions. R package versio 0.4
48. van Swieten JC, Koudstaal PJ, Visser MC et al (1988) Interobserver agreement for the assessment of handicap in stroke patients. Stroke 19:604–607. https://doi.org/10.1161/01.STR.19.5.604
49. Streiner DL, Norman GR (2011) Correction for multiple testing: is there a resolution? Chest 140:16–18. https://doi.org/10.1378/chest.11-0523
50. Finke C, Prüss H, Heine J et al (2017) Evaluation of Cognitive Deficits and Structural Hippocampal Damage in Encephalitis With Leucine-Rich, Glioma-Inactivated 1 Antibodies. JAMA Neurol 74:50–59. https://doi.org/10.1001/jamaneurol.2016.4226
51. Visser PJ, Verhey FRJ, Hofman PaM et al (2002) Medial temporal lobe atrophy predicts Alzheimer's disease in patients with minor cognitive impairment. J Neurol Neurosurg Psychiatry 72:491–497. https://doi.org/10.1136/jnnp.72.4.491
52. Finke C, Heine J, Pache F et al (2016) Normal volumes and microstructural integrity of deep gray matter structures in AQP4+ NMOSD. Neurol Neuroimmunol Neuroinflammation 3:e229. https://doi.org/10.1212/NXI.0000000000000229
53. Fornito A, Zalesky A, Breakspear M (2015) The connectomics of brain disorders. Nat Rev Neurosci 16:159–172. https://doi.org/10.1038/nrn3901
54. Gabilondo I, Martínez-Lapiscina EH, Martínez-Heras E et al (2014) Trans-synaptic axonal degeneration in the visual pathway in multiple sclerosis: Axonal Degeneration in MS. Ann Neurol 75:98–107. https://doi.org/10.1002/ana.24030
55. Krohn S, Müller-Jensen L, Kuchling J et al (2024) Persistent cognitive deficits in anti-LGI1 encephalitis are linked to a reorganization of structural brain networks. bioRxiv. https://doi.org/10.1101/2024.03.07.583948
56. von Schwanenflug N, Ramirez-Mahaluf JP, Krohn S et al (2023) Reduced resilience of brain state transitions in anti-N-methyl-D-aspartate receptor encephalitis. Eur J Neurosci 57:568–579. https://doi.org/10.1111/ejn.15901
57. von Schwanenflug N, Krohn S, Heine J et al (2022) State-dependent signatures of anti-N-methyl-d-aspartate receptor encephalitis. Brain Commun 4:fcab298. https://doi.org/10.1093/braincomms/fcab298

58. Monaghan DT, Cotman CW (1985) Distribution of N-methyl-D-aspartate-sensitive L-[3H]glutamate-binding sites in rat brain. J Neurosci Off J Soc Neurosci 5:2909–2919
59. Eichenbaum H (2017) Elements of information processing in hippocampal neuronal activity: Space, time, and memory. The hippocampus from cells to systems: Structure, connectivity, and functional contributions to memory and flexible cognition. Springer International Publishing AG, Cham, pp 69–94
60. Cavanna AE, Trimble MR (2006) The precuneus: a review of its functional anatomy and behavioural correlates. Brain J Neurol 129:564–583. https://doi.org/10.1093/brain/awl004
61. Buckner RL, Andrews-Hanna JR, Schacter DL (2008) The brain's default network: anatomy, function, and relevance to disease. Ann N Y Acad Sci 1124:1–38. https://doi.org/10.1196/annals.1440.011
62. Raichle ME, Snyder AZ (2007) A default mode of brain function: a brief history of an evolving idea. Neuroimage 37:1083–1090. https://doi.org/10.1016/j.neuroimage.2007.02.041. (**discussion 1097-1099**)
63. Utevsky AV, Smith DV, Huettel SA (2014) Precuneus Is a Functional Core of the Default-Mode Network. J Neurosci 34:932–940. https://doi.org/10.1523/JNEUROSCI.4227-13.2014
64. Cai L, Liang Y, Huang H et al (2020) Cerebral functional activity and connectivity changes in anti-N-methyl-D-aspartate receptor encephalitis: a resting-state fMRI study. NeuroImage Clin 25:102189. https://doi.org/10.1016/j.nicl.2020.102189
65. Wegner F, Wilke F, Raab P et al (2014) Anti-leucine rich glioma inactivated 1 protein and anti-N-methyl-D-aspartate receptor encephalitis show distinct patterns of brain glucose metabolism in 18F-fluoro-2-deoxy-d-glucose positron emission tomography. BMC Neurol 14:136. https://doi.org/10.1186/1471-2377-14-136
66. Galovic M, Al-Diwani A, Vivekananda U et al (2023) In vivo N-Methyl-d-Aspartate Receptor (NMDAR) density as assessed using positron emission tomography during recovery from nmdar-antibody encephalitis. JAMA Neurol 80:211–213. https://doi.org/10.1001/jamaneurol.2022.4352
67. Goldberg E, Podell K, Sodickson DK, Fieremans E (2021) The brain after COVID-19: Compensatory neurogenesis or persistent neuroinflammation? eClinicalMedicine. https://doi.org/10.1016/j.eclinm.2020.100684
68. Lu Y, Li X, Geng D et al (2020) Cerebral Micro-Structural Changes in COVID-19 Patients - An MRI-based 3-month Follow-up Study. EClinicalMedicine 25:100484. https://doi.org/10.1016/j.eclinm.2020.100484
69. Stam CJ (2024) Hub overload and failure as a final common pathway in neurological brain network disorders. Netw Neurosci 8:1–23. https://doi.org/10.1162/netn_a_00339
70. Kuchling J, Jurek B, Kents M et al (2023) Impaired functional connectivity of the hippocampus in translational murine models of NMDA-receptor antibody associated neuropsychiatric pathology. Mol Psychiatry. https://doi.org/10.1038/s41380-023-02303-9
71. Stam CJ, van Straaten ECW, Van Dellen E et al (2016) The relation between structural and functional connectivity patterns in complex brain networks. Int J Psychophysiol 103:149–160. https://doi.org/10.1016/j.ijpsycho.2015.02.011
72. Straathof M, Sinke MR, Dijkhuizen RM, Otte WM (2019) A systematic review on the quantitative relationship between structural and functional network connectivity strength in mammalian brains. J Cereb Blood Flow Metab Off J Int Soc Cereb Blood Flow Metab 39:189–209. https://doi.org/10.1177/0271678X18809547
73. Greicius MD, Supekar K, Menon V, Dougherty RF (2009) Resting-state functional connectivity reflects structural connectivity in the default mode network. Cereb Cortex 19:72–78. https://doi.org/10.1093/cercor/bhn059
74. Achard S, Delon-Martin C, Vertes PE et al (2012) Hubs of brain functional networks are radically reorganized in comatose patients. Proc Natl Acad Sci 109:20608–20613. https://doi.org/10.1073/pnas.1208933109
75. Kuchling J, Brandt AU, Paul F, Scheel M (2017) Diffusion tensor imaging for multilevel assessment of the visual pathway: possibilities for personalized outcome prediction in autoimmune disorders of the central nervous system. EPMA J 8:279–294. https://doi.org/10.1007/s13167-017-0102-x
76. Hartung TJ, Cooper G, Jünger V et al (2023) The T1-weighted/T2-weighted ratio as a biomarker of anti-NMDA receptor encephalitis. J Neurol Neurosurg Psychiatry. https://doi.org/10.1136/jnnp-2023-332069
77. Guasp M, Rosa-Justicia M, Muñoz-Lopetegi A et al (2022) Clinical characterisation of patients in the post-acute stage of anti-NMDA receptor encephalitis: a prospective cohort study and comparison with patients with schizophrenia spectrum disorders. Lancet Neurol 21:899–910. https://doi.org/10.1016/S1474-4422(22)00299-X
78. Farquharson S, Tournier J-D, Calamante F et al (2013) White matter fiber tractography: why we need to move beyond DTI. J Neurosurg 118:1367–1377. https://doi.org/10.3171/2013.2.JNS121294
79. Tournier J-D, Calamante F, Connelly A (2013) Determination of the appropriate b value and number of gradient directions for high-angular-resolution diffusion-weighted imaging. NMR Biomed 26:1775–1786. https://doi.org/10.1002/nbm.3017

Authors and Affiliations

André Hechler[1,2] · Joseph Kuchling[3,4] · Leonie Müller-Jensen[3] · Johanna Klag[3] · Friedemann Paul[3,4,5] · Harald Prüss[3,6] · Carsten Finke[1,3]

✉ Carsten Finke
carsten.finke@charite.de

1 Berlin School of Mind and Brain, Humboldt-Universität zu Berlin, Berlin, Germany

2 TUM-Neuroimaging Center, Technische Universitaet Muenchen, Munich, Germany

3 Department of Neurology and Experimental Neurology, Charité, Universitätsmedizin Berlin, Corporate Member of Freie Universität Berlin and Humboldt-Universität zu Berlin, Charitéplatz 1, 10117 Berlin, Germany

4 Experimental and Clinical Research Center, Max Delbrueck Center for Molecular Medicine and Charité, Universitätsmedizin Berlin, Berlin, Germany

5 Neurocure Cluster of Excellence, NeuroCure Clinical Research Center, Charité, Berlin Institute of Health, Universitätsmedizin Berlin, Corporate Member of Freie Universität Berlin, Humboldt-Universität zu Berlin, Berlin, Germany

6 German Center for Neurodegenerative Diseases (DZNE), Berlin, Berlin, Germany